Upon averaging the integrand in the second of the integrals in (A4) over the interval $q_\perp{}^t L \leq x \leq q_\perp{}^t L + 2\pi$, we have

$$g = \frac{1}{2\pi v_t{}^2} \int_0^\infty \frac{dq_\perp{}^l}{[q_{\parallel}{}^2 + (q_\perp{}^l)^2]^2} [q_{\parallel}{}^2 S_{\parallel}{}^2 \cos^2\phi + (q_\perp{}^l)^2 S_\perp{}^2]$$
$$+ \frac{1}{2\pi v_t{}^2} \int_{q_{\parallel}[(1/\alpha)^2-1]^{1/2}}^\infty \frac{dq_\perp{}^t}{[q_{\parallel}{}^2 + (q_\perp{}^t)^2]^2}$$
$$\times [(q_\perp{}^t)^2 S_{\parallel}{}^2 \cos^2\phi + q_{\parallel}{}^2 S_\perp{}^2]. \quad \text{(A5)}$$

Making use of (A5) and an identical expression obtained with the antisymmetric vibrations we find that the contribution from the mixed and combination modes to the asymptotic intensity can be written

$$I_2{}^{A3} + I_2{}^{A4}$$
$$= \pi^{-1} J \sum_{\mathbf{G}_\parallel}{}' \int_0^\infty \frac{dq_\perp{}^t}{[q_{\parallel}{}^2 + (q_\perp{}^t)^2]^2}$$
$$\times [(q_\perp{}^t)^2 S_{\parallel}{}^2 \cos^2\phi + q_{\parallel}{}^2 S_\perp{}^2]|_{q_\parallel = |\mathbf{S}_\parallel - \mathbf{G}_\parallel|}$$
$$+ \alpha^2 \pi^{-1} J \sum_{\mathbf{G}_\parallel}{}' \int_0^\infty \frac{dq_\perp{}^l}{[q_{\parallel}{}^2 + (q_\perp{}^l)^2]^2}$$
$$\times [q_{\parallel}{}^2 S_{\parallel}{}^2 \cos^2\phi + (q_\perp{}^l)^2 S_\perp{}^2]|_{q_\parallel = |\mathbf{S}_\parallel - \mathbf{G}_\parallel|}. \quad \text{(A6)}$$

The evaluation of these integrals together with the results of the first paragraph establishes the equality between the asymptotic value of $I_2(\mathbf{S})$ and $I_2{}^0(\mathbf{S})$.

PHYSICAL REVIEW VOLUME 153, NUMBER 3 15 JANUARY 1967

Electron Viscosity and Ultrasonic Attenuation in Noble Metals

L. H. HALL
University of California, Santa Barbara, California
(Received 18 July 1966)

Low-temperature absolute ultrasonic attenuations have been observed in silver and copper which are higher than free-electron predictions by a factor of 1.8. Since the real Fermi surfaces of the noble metals are now well enough known to be taken into account, we have formulated expressions for the viscosity tensor of a nonisotropic Bloch electron gas and, in a relaxation-time approximation, deduced detailed formulas for the case of the metals Ag, Au, and Cu, which conform to cubic symmetry. The nondynamical deviations from spherical symmetry do not account for the high observed attenuations, but they do create a marked anisotropy in the viscosity tensor. The electron deformation potential probably contributes significantly.

I. INTRODUCTION

FREE-ELECTRON theory of ultrasonic attenuation in metals does not square quantitatively with the experimental data for the noble metals. For polycrystalline silver and longitudinal waves of frequency ~40 kc/sec, Lax[1] has found that the observational value of the ratio of attenuation coefficient to electric conductivity (α/σ) exceeds the free-electron value by a factor of ~1.8. Recently, Kolouch and McCarthy[2] have noted a similar factor in the case of single-crystal copper for sound of frequency ~40 Mc/sec, propagated in the [111] direction. On the other hand, earlier measurements by Bömmel[3] and also by Gibbon[3] of 15 Mc/sec shear waves along a cubic axis in copper, seemingly do agree with the free-electron value.

The initial free-electron discussion of acoustic attenuation was given by Pippard[4] on the assumption of a constant relaxation time. Steinberg[5] and later Bhatia and Moore,[6] examining the collision integral in detail, concluded that where an effective relaxation time for viscosity can be defined, it will be smaller than the corresponding parameter for electrical conductivity, and that proportionality between α and σ will not obtain—a contradiction to observation.

The disparity has been imputed to possible deviations of the real Fermi surface from the free-electron sphere. If the concept of the Fermi surface is considered to embrace the dynamical behavior thereon, then such properties as the effective electron mass and the deformation potential are included, and the preceding supposition may well be correct.

Since the departures of the Fermi surfaces of the noble metals from the free-electron spheres are now quite accurately known, we have thought it worth while to formulate expressions for the viscosity tensor of a nonisotropic Bloch electron gas, and to deduce in detail formulas for the case of the noble metals, Ag, Au, and Cu, which conform to cubic symmetry. We do this in the approximation of the Boltzmann transport equation with relaxation time essentially constant, but with provision for a limited anisotropy. We can take

[1] E. Lax, Technical Report No. XVII, 1959 (unpublished).
[2] R. J. Kolouch and K. A. McCarthy, Phys. Rev. **139**, A700 (1965).
[3] W. P. Mason, *Physical Acoustics and the Properties of Solids* (D. Van Nostrand Company, Inc., Princeton, New Jersey, 1958), p. 322.
[4] A. B. Pippard, Phil. Mag. **41**, 1104 (1955).
[5] M. S. Steinberg, Phys. Rev. **109**, 1486 (1958).
[6] A. B. Bhatia and R. A. Moore, Phys. Rev. **121**, 1075 (1961).

into account adequately the actual shape of the Fermi surface and place limits on the influence of the anisotropy in τ. However, there is not yet available information on the deformation potential, which apparently is important. In the absence of such dynamical information the present computational scheme might be directed with more reward (but more labor) toward metals whose Fermi surfaces deviate considerably from spherical symmetry.

II. VISCOSITY TENSOR

We calculate the kinetic stress tensor of the electron gas since the viscosity tensor is the coefficient in the term linear in the rate of strain. Let $\mathbf{u}$ be the local acoustic crystal velocity in the laboratory reference frame; $\mathbf{V}=\mathbf{v}-\mathbf{u}$, the electron relative velocity or velocity in a local coordinate system moving with the lattice; $n=n_0+n'$, the electron-particle density; $f(\mathbf{k},\mathbf{r},t)$ is the nonequilibrium electron-distribution function. For acoustic wavelengths long compared with the electron mean free path, the electrons relax toward a local Fermi distribution.[4,7] The acoustic perturbation being small, we write

$$f=f_{\rm loc}{}^0+f^{(1)}.$$

The stress tensor is the momentum flux

$$\mathbf{P}=\frac{1}{4\pi^3}\int m\mathbf{V}\mathbf{V}f_{\rm loc}{}^0d^3k+\frac{1}{4\pi^3}\int m\mathbf{V}\mathbf{V}f^{(1)}d^3k. \quad (1)$$

The relevant equilibrium-distribution function is

$$f_{\rm loc}{}^0=[\exp(\epsilon-\zeta)/kt+1]^{-1}, \quad (2)$$

where the energy ϵ and Fermi energy ζ are local,[7] and each includes a component linear in the strain[8,9] $\mathcal{S}(\mathbf{r},t)$:

$$\begin{aligned}\epsilon&=\epsilon^0(\mathbf{k}-m\mathbf{u}/\hbar)+\lambda(\mathbf{k}):\mathcal{S}\\&=\epsilon^0(\mathbf{k})-\mathbf{v}\cdot m\mathbf{u}+\lambda:\mathcal{S},\end{aligned} \quad (3)$$

where $\epsilon^0(\mathbf{k})$ is the energy function in the unperturbed lattice, and we have used the relation $\partial\epsilon/\partial\mathbf{k}=\hbar\mathbf{v}$.

$$\zeta=\zeta^0(n)+\lambda_F:\mathcal{S}=\zeta^0(n_0)-n'/\mathfrak{N}+\lambda_F:\mathcal{S}; \quad (4)$$

$\lambda(\mathbf{k})$ is the deformation-potential tensor, and $\mathfrak{N}=-(\partial\zeta^0/\partial n_0)^{-1}$, the density of states;

$$\mathfrak{N}=(1/4\pi^3)\int|\partial\epsilon^0/\partial\mathbf{k}|^{-1}dS=(1/4\pi^3\hbar)\int v^{-1}dS, \quad (5)$$

and

$$\lambda_F=(1/4\pi^3\hbar\mathfrak{N})\int\lambda(\mathbf{k})v^{-1}dS. \quad (6)$$

The integrals are over the Fermi surface, the usual first-order approximation $-\partial f^0/\partial\epsilon^0\approx\delta(\epsilon^0-\zeta^0)$ having been employed.

[7] T. Holstein, Phys. Rev. **113**, 479 (1959).
[8] A. I. Akhiezer, M. I. Kaganov, and G. Ia. Liubarskii, Zh. Eksperim. i Teor. Fiz. **32**, 837 (1957) [English transl.: Soviet Phys.—JETP **5**, 685 (1957)].
[9] H. Stoltz, Phys. Status Solidi **3**, 1153 (1963).

We turn to the Boltzmann transport equation to obtain $f^{(1)}$:

$$\mathfrak{D}f=\left[\frac{\partial}{\partial t}+\mathbf{v}\cdot\frac{\partial}{\partial\mathbf{r}}+\dot{\mathbf{k}}\cdot\frac{\partial}{\partial\mathbf{k}}\right]f=\left.\frac{\partial f}{\partial f}\right|_{\rm coll}\approx-\frac{f^{(1)}}{\tau}. \quad (7)$$

To first order,

$$f^{(1)}=-\tau\mathfrak{D}f_{\rm loc}{}^0. \quad (8)$$

With the introduction of the material derivative, $D/Dt\equiv\partial/\partial t+\mathbf{u}\cdot\nabla$,

$$\mathfrak{D}=D/Dt+\mathbf{V}\cdot\nabla+\dot{\mathbf{k}}\cdot\partial/\partial\mathbf{k}. \quad (9)$$

The inhomogeneity of the lattice deformation contributes an effective force on an electron in addition to the electric field generated by the acoustic wave:

$$\hbar\dot{\mathbf{k}}=-e\mathbf{E}-\lambda:\nabla\mathcal{S}. \quad (10)$$

We apply $\mathfrak{D}$ as given in (9) to $f_{\rm loc}{}^0$ in (2), taking note of the $(\mathbf{r},t)$ dependence implied in expressions (3) and (4) for ϵ and ζ, and obtain

$$\begin{aligned}f^{(1)}=-\tau\frac{\partial f_{\rm loc}{}^0}{\partial\epsilon^0}\Big\{&\mathbf{V}\cdot(e\mathbf{E}-\nabla\zeta)-m\mathbf{V}\cdot\mathbf{V}\cdot\nabla\mathbf{u}\\&+(\lambda-\lambda_F):\nabla\mathbf{u}-m\mathbf{V}\cdot\frac{D\mathbf{u}}{Dt}-\frac{1}{\mathfrak{N}}\frac{Dn'}{Dt}\Big\}.\end{aligned} \quad (11)$$

We have been able to replace the electron velocity in the laboratory frame $\mathbf{v}$ by $\mathbf{V}$ wherever the former appears and stay within first-order approximation. Employing the fluid dynamic equations,

$$Dn/Dt=n\nabla\cdot\mathbf{u} \quad (12)$$

$$\begin{aligned}\frac{D\mathbf{u}}{Dt}&=-\frac{1}{\rho}\nabla p+(n_{\rm ion}-n)e\mathbf{E}=-\frac{1}{\rho}\nabla p\\&\quad+\text{2nd-order terms},\end{aligned} \quad (13)$$

where ρ is the crystal density, and

$$D\mathcal{S}/Dt=\nabla\mathbf{u} \quad (14)$$

(irrotational waves), we reach

$$\begin{aligned}f^{(1)}=\tau(\partial f_{\rm loc}{}^0/\partial\epsilon^0)\{&\mathbf{V}\cdot[\nabla\zeta-(m/\rho)\nabla p+e\mathbf{E}]\\&+[m\mathbf{V}\mathbf{V}-(n_0/\mathfrak{N})\mathbf{I}+(\lambda-\lambda_F)]:\nabla\mathbf{u}\}.\end{aligned} \quad (15)$$

We have neglected variation with temperature, which has been shown to be negligible in acoustic perturbation.[10,11]

Only the second square bracket produces a nonvanishing integral for the stress tensor $\mathbf{P}$. Substituting (15) in the second term of (1), setting

$$d^3k=dSd\epsilon|\partial\epsilon/\partial\mathbf{k}|^{-1}=dS\,d\epsilon V^{-1}\hbar^{-1}$$

and again invoking $-\partial f_{\rm loc}{}^0/\partial\epsilon^0\approx\delta(\epsilon^0-\zeta^0)$, we obtain

[10] M. S. Steinberg, Phys. Rev. **111**, 425 (1958).
[11] L. H. Hall, Phys. Rev. **136**, A1136 (1964).

for the viscosity tensor

$$\boldsymbol{\eta}=\left\{\frac{\tau m^2}{4\pi^3\hbar}\int \mathbf{VVVV}V^{-1}dS-\frac{\tau m n_0}{4\pi^3\hbar\mathfrak{N}}\int \mathbf{VV}V^{-1}dS\mathbf{I}\right.$$
$$\left.+\frac{\tau m}{4\pi^3\hbar}\int \mathbf{VV}(\lambda-\lambda_F)V^{-1}dS\right\}. \quad (16a)$$

III. CUBIC SYMMETRY: NOBLE METALS

The noble metals, silver, gold, and copper, crystallize in the face-centered-cubic lattice. In cubic symmetry there are but three distinctive components in the viscosity tensor. We compute components

$$\eta_{1111}\equiv\eta_{11},\quad \eta_{1122}\equiv\eta_{12},\quad \eta_{1212}\equiv\eta_{66}=\eta_{44}=\eta_{2323}$$

in a rectangular coordinate system with axes parallel to the crystallographic axes.

For comparison of theoretical with experimental results, we shall require also the electrical-conductivity tensor $\sigma=\sigma_{11}\mathbf{I}$ (a scalar in the cubic system).

Detailed information on the Fermi-surface parameters is available from studies of several magnetic-resonance effects: de Haas–van Alphen,[12,13] magnetoacoustic,[14,15] and cyclotron resonance.[16] We are in a position therefore to make a computation of the first two integrals required for each of the viscosity components. The third integral, dependent on the deformation potential, is inaccessible at present.

With the omission of the third term, the following anatomy exists:

$$\eta_{11}=\eta_{11}'-\eta_1;\quad \eta_{12}=\eta_{12}'-\eta_1;\quad \eta_{44}=\eta_{12}', \quad (16b)$$

where

$$\eta_{11}'=\frac{\tau m^2}{4\pi^3\hbar}\int V_1^4V^{-1}dS, \quad (17)$$

$$\eta_{12}'=\frac{\tau m^2}{4\pi^3\hbar}\int V_1^2V_2^2V^{-1}dS, \quad (18)$$

$$\eta_1=\frac{\tau m n_0}{4\pi^3\hbar\mathfrak{N}}\int V_1^2V^{-1}dS, \quad (19)$$

$$\mathfrak{N}=\frac{1}{4\pi^3\hbar}\int V^{-1}dS. \quad (20)$$

We therefore have these four integrals to evaluate, and in addition a fifth:

$$\sigma=\frac{\tau e^2}{4\pi^3\hbar}\int V_1^2V^{-1}dS. \quad (21)$$

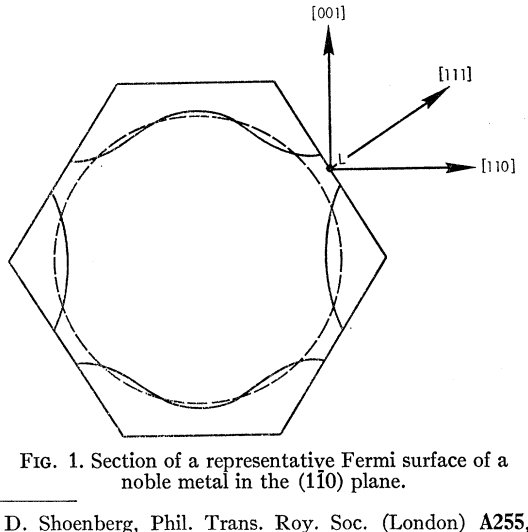

FIG. 1. Section of a representative Fermi surface of a noble metal in the (1$\bar{1}$0) plane.

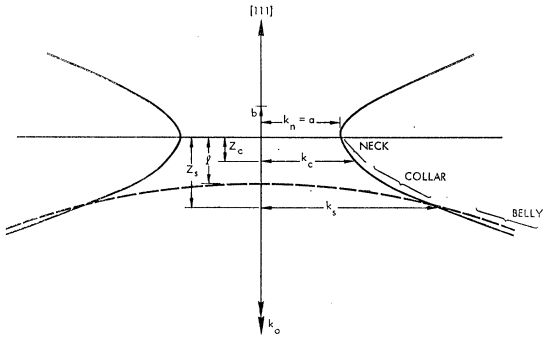

FIG. 2. Section of Fermi surface at a hyperboloidal neck.

IV. FERMI SURFACE

The Fermi shape common to Ag, Au, and Cu comprises a nearly spherical portion (the "belly") with necks in the eight [111] directions, which contact the hexagonal faces of the Brillouin zone, as indicated in Fig. 1. Belly deviations from sphericity are, on the average, within a few percent of the free-electron radius for each metal. Accordingly, for the integral over the belly we use a free-electron sphere less integrals over the eight caps which underlie the necks. Recent de Haas–van Alphen data indicate that belly effective masses for Ag and Au are probably within a few percent of the free-electron values, which implies a like agreement for the belly Fermi velocities. The belly effective mass for Cu, however, seems to be distinctly higher than the free value; we use as an average $m_b/m\approx\frac{4}{3}$ and correspondingly for the ratio of belly Fermi velocity to free electron Fermi velocity, $v_b/v_0\approx\frac{3}{4}$.

The de Haas–van Alphen studies show that the neck shape conforms well to a hyperboloid of revolution,

[12] D. Shoenberg, Phil. Trans. Roy. Soc. (London) **A255**, 85 (1962); D. J. Roaf, *ibid.* **A255**, 135 (1962).
[13] A. S. Joseph and A. C. Thorsen, Phys. Rev. **134**, A979 (1964); **138**, A1159 (1965); A. S. Joseph, A. C. Thorsen, and F. A. Blum, *ibid.* **140**, A2046 (1965).
[14] R. W. Morse, A. Myers, and T. C. Walker, Phys. Rev. Letters 4, 605 (1960).
[15] H. V. Bohm and V. J. Easterling, Phys. Rev. **128**, 1021 (1962).
[16] A. F. Kip, D. N. Langenberg, and T. W. Moore, Phys. Rev. **124**, 359 (1961); J. F. Koch, R. A. Stradling, and A. F. Kip, *ibid.* **133**, A240 (1964).

TABLE I. Fermi-surface parameters. All surface dimensions are stated in momentum units of 10^{-19} g cm sec^{-1}. Symbols refer to labeling in Fig. 2.

	k_0	l	$\bar{m}_b/m$	m_t/m	m_l/m	$k_n=a$	b	k_s	k_c	z_s	z_c
Ag	1.27	0.14	1	0.39	0.12	0.173	0.096	0.41	0.28	0.21	0.125
Au	1.27	0.14	1	0.29	0.123	0.226	0.146	0.38	0.28	0.20	0.103
Cu	1.44	0.15	1.33	0.45	0.177	0.271	0.170	0.44	0.35	0.22	0.135

with the axis in a [111] direction. Joseph and Thoreson[13] find their data for the necks fitted within a few percent by an effective-mass approximation for $\epsilon^0(\mathbf{k})$,

$$\epsilon^0=\epsilon_L+\frac{\hbar^2k_1^2}{2m_t}+\frac{\hbar^2k_2^2}{2m_t}-\frac{\hbar^2k_3^2}{2m_l}, \tag{22}$$

in a coordinate system with the z axis along the [111] direction and the origin at L, the point of intersection with the Brillouin face. m_t is the transverse effective mass and m_l is the longitudinal effective mass. ϵ_L is the electron energy at L. We utilize (22) to provide both the Fermi surface and, through its gradient, the electron velocity on the Fermi surface. Equation (22) refers to a stationary, unstressed crystal. For an unstressed crystal in small motion, we expect the replacement $\epsilon^0(\mathbf{k})\rightarrow\epsilon^0(\mathbf{k}-m\mathbf{u}/\hbar)$, whose gradient would yield the relative velocity $\mathbf{V}$. However, we require the Fermi velocity to only zeroth order since the viscosity integrals are multiplied by the first-order factor $\nabla\mathbf{u}$. We may therefore use (22) directly and regard its gradient as the relative velocity $\mathbf{V}$.

Figure 2 is a sketch of the neck region. Table I contains parameter values required for the integrations. Neck data and inferences therefrom are most accurate at the top of the neck, where it intersects the zone face. While the hyperboloid determined by (22) does not join the belly smoothly as we rightly expect it to do, such a discontinuity is of little consequence in the integration. However, the computed ratio of the neck velocity to the belly velocity at the conjunction is high, approximately 1.6 for Ag and Au (only 1.1 for Cu). We have therefore made alternative computations—one tolerating the mismatch, a second with a conciliating expedient: Noting that the Fermi velocity on the neck increases with proximity to the belly, we accept the increase provided by (22) until it reaches the belly value; thereafter we hold the magnitude constant and retain only the directional variation. The lower section of the neck so defined will be labeled the "collar" for reference. The Fermi surface for purpose of integration assumes the anatomy: sphere, caps, necks, and collars. Providing the neck with a collar diminishes the viscosities on the order of 10%.

Effective relaxation times for neck and belly differ.[17,18] For low-temperature impurity scattering $\tau_{ni}>\tau_{bi}$, whereas for phonon scattering $\tau_{np}<\tau_{bp}$. In the case of copper, Deaton and Gavenda[19] estimate from their magneto-acoustic data that relaxation on the neck is several times slower than on the belly. We have made exploratory computations using successively $\tau_n/\tau_b=1, 2, \frac{1}{2}$. The variations so produced are also of the order of ±10%.

[17] J. M. Ziman, Phys. Rev. **121**, 1320 (1961).
[18] V. Heine, Phil. Mag. **12**, 53 (1965).
[19] B. C. Deaton and J. D. Gavenda, Phys. Rev. **129**, 1990 (1963).

V. COMPUTATION OF INTEGRALS

Integration over the sphere excepted, the various integrals (17)–(21), formulated in terms of crystallographic axes, are most readily evaluated by a transformation to a coordinate system with z axis along the [111] direction. For the most symmetrical orientation, the direction cosines of such neck axes relative to the crystallographic ones are

$$\alpha_1=(\sqrt{3}+3)/6,\quad \alpha_2=(\sqrt{3}-3)/6,\quad \alpha_3=-2\sqrt{3}/6;$$
$$\beta_1=(\sqrt{3}-3)/6,\quad \beta_2=(\sqrt{3}+3)/6,\quad \beta_3=-2\sqrt{3}/6;$$
$$\gamma_1=\gamma_2=\gamma_3=2\sqrt{3}/6.$$

If we denote the velocity components along the new axes by U_1, U_2, U_3, we have, for example (to clarify the notation),

$$V_1=U_1\alpha_1+U_2\beta_1+U_3\gamma_1. \tag{23}$$

Upon transformation and exploitation of rotational symmetry the integrals become

$$\eta_{11}'=\frac{\tau m^2}{4\pi^3\hbar}\frac{1}{36}\left\{16\int U_1^4U^{-1}dS+4\int U_3^4U^{-1}dS+48\int U_1^2U_3^2U^{-1}dS\right\}, \tag{24}$$

$$\eta_{12}'=\frac{\tau m^2}{4\pi^3\hbar}\frac{1}{36}\left\{8\int U_1^4U^{-1}dS+4\int U_3^4U^{-1}dS\right\}, \tag{25}$$

$$\sigma=\frac{\tau e^2}{4\pi^3\hbar}\frac{1}{3}\int UdS.$$

Differentiating $\epsilon(\mathbf{k})$ in (22), we have for the velocity components

$$U_1=hk_1/m_t,\quad U_2=hk_2/m_t,\quad U_3=-hk_3/m_l. \tag{26}$$

Over a cap, spherical coordinates are employed; over neck and collar, cylindrical coordinates. The integrations are elementary but laborious; the results appear in the Appendix.

Application to silver, with the contributions of the various regions separately displayed, is given below.

TABLE II. Viscosity terms and electrical conductivity. The tabulated numerical values are in fact the following ratios: $\sigma\times 4\pi^2\hbar/\tau e^2k_0^2v_0$, $\eta_{11}'/\sigma(m/e)^2v_0^2$, $\eta_{12}'/\sigma(m/e)^2v_0^2$, and $\eta_1/\sigma(m/e)^2v_0^2$.

	σ	η_{11}'	η_{12}'	η_1
Ag	1.31	0.63	0.17	0.31
Au	1.32	0.67	0.17	0.32
Cu	1.01	0.44	0.13	0.25
Free-electron gas	1.33	0.60	0.20	0.33

Numbers in the square brackets refer in order to sphere, caps, collars, and necks.

$$\eta_{11}'=(\tau m^2/4\pi^2\hbar)k_0^2v_0^3[0.800-0.113+0.107+0.033], \quad (27)$$

$$\eta_{12}'=(\tau m^2/4\pi^2\hbar)k_0^2v_0^3[0.267-0.085+0.030+0.008], \quad (28)$$

$$\mathfrak{N}=(1/4\pi^2\hbar)k_0^2v_0^{-1}[4.000-0.852+0.541+0.613], \quad (29)$$

$$\sigma=(\tau e^2/4\pi^2\hbar)k_0^2v_0[1.333-0.284+0.179+0.086], \quad (30)$$

$$\eta_1=\sigma(m/e^2)\hbar k_0v_0[0.312]. \quad (31)$$

k_0 and v_0 are the free-electron Fermi radius and Fermi velocity. We have replaced U_0 by the zero-order Fermi velocity v_0.

VI. VISCOUS ATTENUATION

Comparison of theory with experiment occurs through examination of the ratio of attenuation coefficient to electrical conductivity α/σ in the two cases. Since the viscous dissipation is proportional to the viscosity, we compute the ratio η/σ. We shall isolate the distinctive numerical factor as indicated for silver:

$$\eta_{11}'/\sigma(m/e)^2v_0^2=[0.63], \quad (32)$$

$$\eta_{12}'/\sigma(m/e)^2v_0^2=[0.17], \quad (33)$$

$$\eta_1/\sigma(m/e)^2v_0^2=[0.31]. \quad (34)$$

The ratios for the three metals, and for the free-electron model as well, are presented in Table II.

The viscous amplitude attenuation coefficient for longitudinal plane waves is

$$\alpha=(\omega^2/2\rho c)\eta_{\text{long}}, \quad (35)$$

where η_{long} is the effective longitudinal viscosity in the direction of propagation. Similarly, for shear plane waves,

$$\alpha=(\omega^2/2\rho c)\eta_{\text{shear}}, \quad (36)$$

where $\eta_{\text{shear}}\equiv\eta_s$ is the effective shear viscosity for the direction of propagation.

A. Polycrystalline Materials

Under acoustic irradiation, polycrystalline materials of sufficiently small grain size behave isotropically; for such media

$$\eta_{\text{long}}=(\bar{\eta}_v+\tfrac{4}{3}\bar{\eta}_s), \quad (37)$$

where $\bar{\eta}_s$ is the average coefficient of shear viscosity and $\bar{\eta}_v$ is that of volume viscosity. Averages have been computed in elasticity theory for the corresponding elastic moduli. There, various assumptions have been employed; e.g., uniform local strain (Voigt), uniform local stress (Reuss).[20] Mason[21] has given a simple deduction which leads to the Voigt results. Voigt averages have been shown to provide an upper limit and Reuss, a lower. For cubic structures, however, the two averages coincide for the bulk or volume modulus. For the shear viscous coefficient we shall choose the Voigt averaging. It gives a value approximately equal to the free-electron one, a plausible result. The Reuss averaging gives, on the contrary, the rather implausible value of only 0.6 times the free-electron one. Further, the condition of local uniform rate of strain, the analog of the elastic condition of uniform local strain, appears proper.

The average shear viscosity is then

$$\bar{\eta}_s=\tfrac{1}{5}(\eta_{11}-\eta_{12}+3\eta_{44}). \quad (38)$$

The average volume viscosity is

$$\bar{\eta}_v=\tfrac{1}{3}(\eta_{11}+2\eta_{12}). \quad (39)$$

Table III contains the average viscosities for the three metals along with the associated ultrasonic attenuations.

TABLE III. Polycrystalline materials. Viscosity coefficients, i.e., ratios $\eta/\sigma(m/e)^2v_0^2$ and associated ultrasonic attenuations.

	$\bar{\eta}_s$	$\bar{\eta}_v$	$\bar{\eta}_{\text{long}}$	$\alpha/\alpha_{\text{free}}$
Ag	0.19	$\sim$0	0.26	0.95
Au	0.20	$\sim$0	0.27	1.0
Cu	0.14	$\sim$0	0.19	0.7
Free-electron gas	0.20	0	0.267	1

B. Single Crystals

For plane waves propagating in the [111] direction, the relevant viscosity coefficients are, for longitudinal waves,[16]

$$\eta_{\text{long}}^{[111]}=\tfrac{1}{3}(\eta_{11}+2\eta_{12}+4\eta_{44}), \quad (40)$$

and for shear waves

$$\eta_{\text{shear}}^{[111]}=\tfrac{1}{3}(\eta_{11}-\eta_{12}+\eta_{44}). \quad (41)$$

For propagation in the [100] direction,

$$\eta_{\text{long}}^{[100]}=\eta_{11}, \quad (42)$$

and

$$\eta_{\text{shear}}^{[100]}=\eta_{44}. \quad (43)$$

[20] H. B. Huntington, in *Solid State Physics*, edited by F. Seitz and D. Turnbull (Academic Press Inc., New York, 1958), Vol. 7, pp. 213, 317, 318.

[21] W. P. Mason, *Piezoelectric Crystals and Their Application to Ultrasonics* (D. Van Nostrand Company, Inc., Princeton, New Jersey, 1950), pp. 414–416.

TABLE IV. Single crystals. Viscosity coefficients $[\eta/\sigma(m/e)^2v_0^2]$ and associated ultrasonic attenuations.

	[111] direction		[100] direction			
	η_{long}	$\alpha/\alpha_{\text{free}}$	η_{long}	$\alpha/\alpha_{\text{free}}$	η_{shear}	$\alpha/\alpha_{\text{free}}$
Ag	0.24	0.9	0.32	1.2	0.17	0.85
Au	0.24	0.9	0.35	1.3	0.17	0.85
Cu	0.16	0.6	0.19	0.7	0.13	0.65
Free-electron gas	0.267	1	0.267	1	0.20	1

The values of the above viscosities and associated attenuations appear in Table IV.

VII. CONCLUSIONS

Geometrically, the Fermi surface necks do not account for the high ultrasonic attenuations observed in the noble metals, both because of their small size and the variation of their influence with crystalline direction.

However, through the mediation of the necks, the crystalline anisotropy is reflected distinctly in the viscosity tensor. Such marked anisotropy has indeed been observed in tin crystals.[22]

The acoustic frequencies employed by Kolouch and McCarthy for copper lie above the viscous regime (acoustic wavelength > electron mean free path); nevertheless, their data by free-electron theory point to the same excess attenuation factor for low as for high frequencies. An earlier found agreement between the Bömmel and Gibbon copper measurements and free-electron values was deceptive: It was based on the use of the free-electron mass. When the now known large belly effective mass of copper is employed, computed attenuation values are decidedly lowered and agreement lost.

If our framework is valid, the deformation potential $\mathfrak{A}$ must contribute importantly to electron viscosity.

ACKNOWLEDGMENT

I am grateful to Stanley Kranzler for lightening the burden of computation.

APPENDIX

The transport integrals indicated in (20), (24), and (25) evaluated over the various regions are as follows (subscript b denotes belly value):

Neck

$$\eta_{11}'=\frac{\tau_n m^2}{4\pi^2\hbar}k_b^2v_b^3\left(\frac{k_n}{k_b}\right)^2\left(\frac{v_n}{v_b}\right)^3\left\{\frac{1}{45}\left(\frac{m_l}{m_t}\right)^{1/2}A+\frac{2}{45}\left(\frac{m_t}{m_l}\right)^{3/2}B+\frac{4}{45}C\right\} \tag{A1}$$

$$\eta_{12}'=\frac{\tau_n m^2}{4\pi^2\hbar}k_b^2v_b^3\left(\frac{k_n}{k_b}\right)^2\left(\frac{v_n}{v_b}\right)^3\left\{\frac{1}{90}\left(\frac{m_l}{m_t}\right)^{1/2}A+\frac{2}{45}\left(\frac{m_t}{m_l}\right)^{3/2}B\right\}, \tag{A2}$$

where, upon setting

$$K_c=[(k_c^2/k_n^2)-1]^{1/2},\quad A=3K_c^5+10K_c^3+15K_c,\quad B=K_c^5,\quad C=K_c^3(3k_c^2/k_n^2+2).$$

$$\sigma=\frac{\tau_n e^2}{4\pi^2\hbar}k_b^2v_b\left(\frac{k_n}{k_b}\right)^2\left(\frac{v_n}{v_b}\right)\left\{\frac{2}{9}\left(\frac{m_l}{m_t}\right)^{1/2}D+\frac{2}{9}\left(\frac{m_t}{m_l}\right)^{1/2}E\right\}, \tag{A3}$$

where

$$D=K_c[(k_c^2/k_n^2)+2]^{1/2};\quad E=K_c^3.$$

$$\mathfrak{A}=\frac{1}{4\pi^2\hbar}k_b^2v_b^{-1}\left(\frac{k_n}{k_b}\right)^2\left(\frac{v_n}{v_b}\right)^{-1}\left\{2\left(\frac{m_l}{m_t}\right)^{1/2}K_c\right\}. \tag{A4}$$

Collar

$$\eta_{11}'=\frac{\tau_c m^2}{4\pi^2\hbar}k_b^2v_b^3\left(\frac{k_n}{k_b}\right)^2\left\{\left(1+\frac{m_l}{m_t}\right)^{1/2}\left[\frac{4}{9}F+\frac{1}{9}G+\frac{4}{3}H\right]\right\}, \tag{A5}$$

$$\eta_{12}'=\frac{\tau_c m^2}{4\pi^2\hbar}k_b^2v_b^3\left(\frac{k_n}{k_b}\right)^2\left\{\left(1+\frac{m_l}{m_t}\right)^{1/2}\left[\frac{2}{9}F+\frac{1}{9}G\right]\right\}, \tag{A6}$$

[22] W. P. Mason and H. E. Bömmel, J. Acoust. Soc. Am. 28, 930 (1956).

where first defining

$$K_s=(k_s^2/k_n^2-1)^{1/2},\quad Q=(1+m_l/m_t)^{-1};\quad A_s=(k_s^2/k_n^2-Q)^{1/2},\quad A_c=(k_c^2/k_n^2-Q)^{1/2};$$

we have

$$F=\frac{3}{4}\left(1+\frac{m_t}{m_l}\right)^{-2}\left\{\left[\frac{1}{2}-\frac{Q^2}{(Q-1)A_s^2}\right]K_sA_s-\left[\frac{1}{2}-\frac{Q^2}{(Q-1)A_c^2}\right]K_cA_c+\frac{(3Q+1)}{2}\ln\left[\frac{A_s+K_s}{A_c+K_c}\right]\right\},$$

$$G=2\left(1+\frac{m_l}{m_t}\right)^{-2}\left\{\frac{K_c^2}{(Q-1)A_c}-\frac{K_s^2}{(Q-1)A_s}+\frac{A_sK_s}{2(Q-1)}\left[2\left(\frac{k_s}{k_n}\right)^2+3Q-5\right]\right.$$

$$\left.-\frac{A_cK_c}{2(Q-1)}\left[2\left(\frac{k_c}{k_n}\right)^2+3Q-5\right]+\tfrac{3}{2}(Q-1)\ln\left[\frac{A_s+K_s}{A_c+K_c}\right]\right\},\quad\text{(A7)}$$

$$H=\left(2+\frac{m_l}{m_t}+\frac{m_t}{m_l}\right)^{-1}\left\{\left[\frac{1}{2}+\frac{Q}{A_s^2}\right]A_sK_s-\left[\frac{1}{2}+\frac{Q}{A_c^2}\right]A_cK_c+\tfrac{1}{2}(3Q-1)\ln\left[\frac{A_s+K_s}{A_c+K_c}\right]\right\}.$$

$$\sigma=\frac{\tau_c e^2}{4\pi^2\hbar}k_b^2v_b\left(\frac{k_n}{k_b}\right)^2\left\{\left(1+\frac{m_l}{m_t}\right)^{1/2}J\right\},$$

where

$$J=\left(1+\frac{m_t}{m_l}\right)^{-1}\left\{\frac{A_sK_s}{2}-\frac{A_cK_c}{2}+\tfrac{1}{2}(Q+1)\ln\left[\frac{A_s+K_s}{A_c+K_c}\right]\right\}.$$

$$\mathfrak{R}=\frac{1}{4\pi^2\hbar}k_b^2v_b^{-1}\left(\frac{k_n}{k_b}\right)^2\left\{\left(1+\frac{m_l}{m_t}\right)^{1/2}L\right\},\quad\text{(A8)}$$

where

$$L=\left\{\frac{A_sK_s}{2}-\frac{A_cK_c}{2}+\tfrac{1}{2}(1-Q)\ln\left[\frac{A_s+K_s}{A_c+K_c}\right]\right\}.$$

Cap

$$\eta_{11}'=(\tau_bm^2/4\pi^2\hbar)k_b^2v_b^3\{(1/90)[18\sin^4\theta\cos\theta-48\cos\theta+16\cos^3\theta+36-4\cos^5\theta]\},\quad\text{(A9)}$$

$$\eta_{12}'=(\tau_bm^2/4\pi^2\hbar)k_b^2v_b^3\{(1/90)[-3\sin^4\theta\cos\theta-12\cos\theta+4\cos^3\theta+12-4\cos^5\theta]\},\quad\text{(A10)}$$

$$\sigma=(\tau_be^2/4\pi^2\hbar)k_b^2v_b\{\tfrac{2}{3}(1-\cos\theta)\},\quad\text{(A11)}$$

$$\mathfrak{R}=(1/4\pi^2\hbar)k_b^2v_b^{-1}\{2(1-\cos\theta)\}.\quad\text{(A12)}$$

Sphere

$$\eta_{11}'=(\tau_bm^2/4\pi^2\hbar)k_b^2v_b^3\{\tfrac{4}{5}\},\quad\text{(A13)}$$

$$\eta_{12}'=(\tau_bm^2/4\pi^2\hbar)k_b^2v_b^3\{4/15\},\quad\text{(A14)}$$

$$\sigma=(\tau_be^2/4\pi^2\hbar)k_b^2v_b\{\tfrac{4}{3}\},\quad\text{(A15)}$$

$$\mathfrak{R}=(1/4\pi^2\hbar)k_b^2v_b^{-1}\{4\}.\quad\text{(A16)}$$

For the free-electron model, we also have

$$\eta_1=(\tau m^2/4\pi^2\hbar)k_0^2v_0^3\{4/9\}.\quad\text{(A17)}$$

For the noble metals we can take $n_0=(1/3\pi^2)k_0^2$. The final formulas are obtained by appropriate summing.